Intragenic and intergenic suppression of the *Escherichia coli* ATP synthase subunit *a* mutation of Gly-213 to Asn: functional interactions between residues in the proton transport site

Phillip H. KUO and Robert K. NAKAMOTO[1]

University of Virginia, Department of Molecular Physiology and Biological Physics, P.O. Box 10011, Charlottesville, VA 22906-0011, U.S.A.

Subunit *a* of the ATP synthase F_o sector contains a transmembrane helix that interacts with subunit *c* and is critical for H^+ transport activity. From a cysteine scan in the region around the essential subunit *a* residue, Arg-210, we found that the replacement of *a*Gly-213 greatly attenuated ATP hydrolysis, ATP-dependent proton pumping and $\Delta\mu_H+$-dependent ATP synthesis. Various amino acid substitutions caused similar effects, suggesting that functional perturbations were caused by altering the environment or conformation of *a*Arg-210. *a*G213N, which was particularly severe in effect, was suppressed by two second-site mutations, *a*L251V and *c*D61E. These mutations restored efficient coupling; the latter also increased ATP-dependent proton transport rates. These results were consistent with the proposed functional interaction between *a*Arg-210 and *c*Asp-61, the likely carrier of the transported proton. From Arrhenius analysis of steady-state ATP hydrolytic activity, the transport mutants had large increases in the transition-state enthalpic and entropic parameters. Linear isokinetic relationships demonstrate that the transport mechanism is coupled to the rate-limiting catalytic transition-state step, which we have previously shown to involve the rotation of the γ subunit in multi-site, co-operative catalysis.

Key words: coupling, isokinetic analysis, rotational catalysis, transition state.

INTRODUCTION

The eubacterial F_oF_1 ATP synthase contains eight different subunits with a total molecular mass of over 500 kDa (reviewed in [1–4]). Five of the subunits are found in the soluble F_1 sector with a stoichiometry of $\alpha_3\beta_3\gamma\delta\epsilon$, and three are in the membrane-associated F_o sector, ab_2c_{10-12}. The catalytic domain, whose structure was solved by X-ray crystallography [5], consists of $\alpha_3\beta_3\gamma$ with one active site in each β subunit with some contribution from the neighbouring α subunit. Rotation of the γ subunit relative to the $\alpha_3\beta_3$ hexamer has been shown to have an integral role in steady-state turnover [6–9].

The transport domain is less well defined; however, the high-resolution structures of the isolated protonated and unprotonated *c* subunit in solution have been achieved by NMR techniques [10]. Furthermore, Stock et al. [11] obtained a 3.9 Å resolution map of the partial mitochondrial complex from yeast, which included a decamer of *c* subunits arranged in the predicted ring [6,12–14] with the C-terminal helix on the perimeter. Although the resolution did not permit the assignment of side chains, the electron densities of the yeast map were similar to the hairpin structure solved by NMR. Unfortunately, subunit *a*, which is also required for transport, was not represented in the crystal structure.

Importantly, recent evidence now demonstrates that the *c* subunits also undergo ATPase-dependent rotation [15], which is consistent with several models of transport [12,16–18]. Nevertheless, because biochemical and structural analyses of the extremely hydrophobic F_o sector are difficult, there is considerably less experimental evidence related to the transport mechanism. Despite these difficulties, considerable information about structure–function relationships in F_o has been obtained by mutagenic approaches. In this manner several functionally important residues in F_o have been identified. The carboxylic acid of *c*Asp-61, which is located near the middle of the bilayer, is essential for transport function [19]. Several residues in proximity to *c*Asp-61 seem to create an environment that defines the properties of the carboxylic acid that are required for proton transport [10,20–25]. In subunit *a*, the replacement of many residues disrupts transport function; however, only one, *a*Arg-210, has proved to be essential for coupled transport because any replacement, including Lys, causes complete loss of function [26–29]. Significantly, swapping the Arg with *a*Gln-252 to create a double mutant, *a*R210Q/*a*Q252R, retains a small amount of activity, suggesting that the position of *a*Gln-252 is very close to that of *a*Arg-210 [28]. Several amino acid replacements of *a*Gln-252 by itself also cause perturbations of the transport mechanism [12,28,30].

Mutational studies have also shown functional interaction between *a* and *c* subunits. Fraga et al. [21] identified several second-site mutations that genetically suppressed the *c* subunit double mutation, *c*A24D/*c*D61G. Whereas some mapped near *c*Asp-61, others were found in subunit *a* in the putative fourth helix [31,32] which resulted in changes in residues *a*Ala-217, *a*Ile-221 and *a*Leu-224. The two transmembrane helices containing these residues probably interact physically because disulphide

Abbreviations used: ACMA, 9-amino-6-chloro-2-methoxyacridine; CCCP, carbonyl cyanide *m*-chlorophenylhydrazone; FLAG, Asp-Tyr-Lys-Asp-Asp-Asp-Asp-Lys; LB, Luria–Bertani. Mutations are indicated by subunit name, wild-type residue (single-letter amino acid code), residue number and mutant residue; for example, *a*R210Q is arginine 210 in subunit *a* replaced by glutamine.

[1] To whom correspondence should be addressed (e-mail rkn3c@virginia.edu).

bonds could be induced between various pairs of cysteine replacements [33].

A critical question is whether *c*Asp-61 and *a*Arg-210 interact physically and functionally, as has been suggested in many models for transport [10,12,16,29]. This is a difficult question to answer because all substitutions of *a*Arg-210 are null mutations. As an alternative, we used cysteine scanning to search for amino acid changes near *a*Arg-210 that affected transport function, presumably by perturbing the environment around the arginine residue or by causing a shift in its conformation. We report here that such effects were found by replacing the proximal *a*Gly-213. Significantly, an *a*Gly-213 → Asn mutation was suppressed by the second-site mutations *a*L251V or *c*D61E. These results indicate functional interactions between *a*Arg-210, *a*Gln-252 and *c*Asp-61 in the transport mechanism and thereby provide evidence for the constituents of the transport site.

EXPERIMENTAL

Strains and plasmids

The expression plasmid pACWU1.2 [34] carries the eight structural genes for the F_oF_1 complex and complements the *unc* operon-deleted *Escherichia coli* strain DK8 [*bglR*, *thi-1*, *rel-1*, *HfrPO1*, Δ(*uncB-uncC*) *ilv::Tn10*] [35]. This strain grows on defined minimal medium containing 15 mM sodium succinate as a sole carbon source [36]. The FLAG epitope (Asp-Tyr-Lys-Asp-Asp-Asp-Asp-Lys), added to the N-terminus of the β subunit for purification purposes, does not affect the assembly or functional characteristics of the enzyme [34,37]. For the cysteine scanning, the cysteine-less F_oF_1 complex with the FLAG epitope was expressed from plasmid pACWU1.2/β-FLAG/ΔCys [34]. To assist mutagenesis and cloning, several subclones were used. The subclone pBKSaHB was derived from pBluescriptII KS+ (Stratagene, La Jolla, CA, U.S.A.) and contained the *unc* operon from the *Hin*dIII restriction site upstream of *uncB* (subunit *a* gene) to the *Bam*HI site in *uncB* in codon 235 (this subclone was used for the introduction of *uncB* cysteine mutations). The native *Bam*HI site in codon 29 of *uncB* was eliminated by introducing a silent mutation [34]. pBH-RI was derived from pBluescript II KS^+ (Stratagene) and contained most of *uncB* and all of *uncE*, *uncF* and *uncH* (*a*, *c*, *b* and δ subunit genes respectively) between the *Bam*HI and *Eco*RI sites.

Molecular biology procedures

Molecular biology procedures were performed in accordance with manufacturers' instructions or as detailed by Sambrook et al. [38]. Restriction and DNA-modifying enzymes were obtained from Roche Molecular Biochemicals (Indianapolis, IN, U.S.A.), Gibco BRL (Rockville, MD, U.S.A.) and New England Biolabs (Beverly, MA, U.S.A.). Site-directed mutagenesis was performed with PCR methodologies [39] with *Pfu* polymerase (Stratagene).

Region-specific random mutations were generated by oligonucleotide-directed mutagenesis with the Stratagene Chameleon Kit. Doped oligonucleotides were synthesized by Integrated DNA Technologies (Coralville, IA, U.S.A.) or Oligos Etc. (Wilsonville, OR, U.S.A.) at 98% fidelity; 98% of the correct base and 0.7% of the other three bases were used for each position, thereby theoretically producing approximately one base change per 80 bp oligonucleotide.

Screening for second-site suppressor mutants

After mutagenesis had been performed as described above, the mutagenized DNA was excised from pBKSaHB with *Hin*dIII and *Bam*HI, or from pBH-RI by *Bam*HI and *Ppu*MI, and ligated back into pACWU1.2 already carrying the *a*G213N mutation for phenotypic screening. Generally, 10^3–10^4 colonies arose from transformation by the mixture of ligated products. The *a*G213N mutant strain grew very slowly with moderate yields in liquid minimal medium containing sodium succinate as a sole carbon source. To enrich the culture with faster-growing strains, the following procedure was used, which was similar to that described by Fraga et al. [21]. Strain DK8 transformed with mutagenized plasmids was incubated overnight in 1 ml of rich Luria–Bertani (LB) medium containing 0.1 mg/ml ampicillin. A 0.2 ml sample of the culture was used to inoculate 5 ml of liquid sodium succinate minimal medium. After 24 h, 0.1 ml was removed and used to inoculate a fresh 5 ml of succinate medium. After 48 h the culture was spread on succinate minimal medium plates and incubated at 37 °C for 4 days. Well-formed colonies were individually picked and grown in liquid LB containing 0.1 mg/ml ampicillin. After isolation of the plasmid, restriction fragments containing the mutagenized region were moved into the original pACWU1.2/*a*G213N to ensure that no mutations outside the desired region were selected. DNA sequencing of both strands over the entire cloned DNA fragment (performed by the University of Virginia Biomolecular Research Facility, Charlottesville, VA, U.S.A.) was used to identify random mutations, the presence of the primary mutation and a lack of any other changes. The resultant plasmids were again transformed into DK8 and tested for growth on succinate minimal plates.

Alternatively, selection was performed by spreading DK8 transformed with a shotgun ligation of the mutagenized restriction fragment into pACWU1.2/*a*G213N on LB/ampicillin plates. Well-isolated colonies were tested on succinate minimal medium plates by incubating them at 37 °C for 4 days.

Membrane preparations

To prepare F_oF_1-containing membrane vesicles, strains were grown at 37 °C until mid-exponential phase in minimal medium containing 0.4% glucose; membranes were isolated as described previously [40]. Protein concentrations were determined by the method of Lowry et al. [41]. The membrane vesicles were finally suspended at 20–40 mg/ml in a buffer consisting of 5 mM Tris/HCl, 70 mM KCl, 0.5 mM dithiothreitol and 55% (v/v) glycerol at pH 8.0. Depletion of F_1 from the membrane preparations was done as described previously [42].

Quantification of F_oF_1 complex in membrane preparations

Determination of the F_1 content in membrane preparations was performed by a quantitative immunoblot assay described previously [43]. Purified F_1 was used as a reference standard. In addition, the amount of subunit *a* in membrane preparations was estimated by immunoblot with anti-subunit *a* rabbit polyclonal antibody [gift from Dr Hiroshi Omote and Dr Masamitsu Futai (Osaka University, Osaka, Japan)]. In this case, subunit *a* bands were revealed by luminescence with the enhanced chemiluminescence (ECL)® kit (Amersham Pharmacia Biotech, Piscataway, NJ, U.S.A.).

Enzymic assays

The formation of an electrochemical gradient of protons was followed by using Acridine Orange at pH 7.5, as described previously [44]. Alternatively, ATP-dependent proton pumping activity in membrane vesicles was measured by using 9-amino-6-chloro-2-methoxyacridine (ACMA) at pH 8.0. The conditions for the ACMA assay were optimized for maximal sensitivity and

are detailed in the legend to Figure 3. ATP hydrolysis rates were determined at 30 °C in a buffer containing 50 mM Hepes/KOH, 10 mM ATP, 5 mM $MgSO_4$ and 1 μM carbonyl cyanide *m*-chlorophenylhydrazone (CCCP), pH 7.5, with 5 mM phosphoenolpyruvate, 50 μg/ml pyruvate kinase and 0.1–0.3 mg/ml membrane protein [45]. For the Arrhenius analysis, the pH was adjusted to 7.5 at the appropriate temperature [43]. ATP synthesis rates were determined at 30 °C as described previously [45]. The concentration of free Mg^{2+} and $MgATP^{2-}$ was calculated by using the algorithm of Fabiato and Fabiato [46].

Materials

ACMA was from Molecular Probes (Eugene, OR, U.S.A.). Hexokinase, ATP, NADH and Acridine Orange were obtained from Sigma Chemicals (St Louis, MO, U.S.A.), and pyruvate kinase was from Roche Molecular Biochemicals. All other reagents were of the highest grade and purity available.

RESULTS

Effects of cysteine replacements in helix 4 of subunit *a*

Mutations were introduced into *uncB* (subunit *a*) on plasmid pACWU1.2 [34] to replace each residue systematically in the putative helix 4, residues 207–228, with cysteine. The mutations were made in a background F_oF_1 complex that was otherwise devoid of cysteine residues (ΔCys [34]) and expressed in strain DK8 (Δ*unc* [35]). For each mutant strain, Figure 1 indicates the ATP-dependent H^+ pumping activity in membrane vesicles, NADH-driven H^+ pumping via electron transport, and oxidative phosphorylation-dependent growth with sodium succinate as a sole carbon source. All values are relative to the ΔCys F_oF_1 strain. Most of the cysteine replacements in the putative helix 4 of subunit *a* had little or no apparent effect on the function of the complex. H^+ pumping driven by NADH provided an indicator of H^+ leak in membrane vesicles, which might be caused by defective association of the F_1 sector with F_o, thus leaving a H^+-conducting pathway. Growth on succinate is a very sensitive assay for the ability to perform net ATP synthesis. As expected, the cysteine replacements of residues *a*Arg-210, *a*Gly-218 and *a*Glu-219 were deleterious to enzyme function. The nearly complete loss of growth on succinate and H^+ pumping for the *a*R210C and *a*E219C mutants and the less severe effects of the *a*Gly-218 mutant were consistent with results reported previously [12,26–29,47,48].

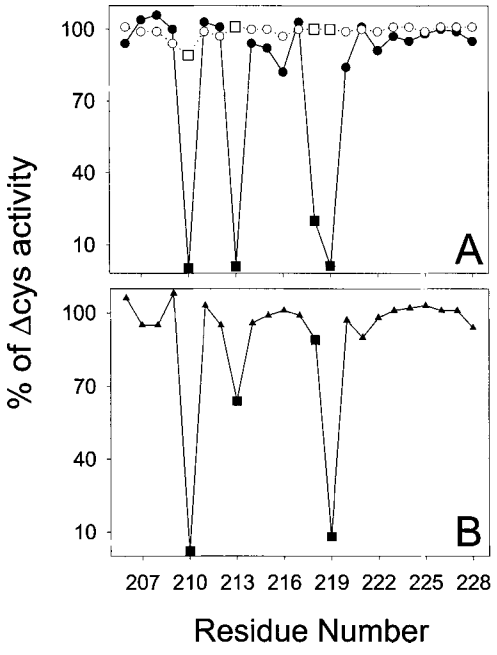

Figure 1 Properties of enzymes with cysteine replacements in the putative helix 4 of subunit *a*

(**A**) ATP-driven (●,■) and NADH-driven H^+ pumping (○,□) were determined by Acridine Orange fluorescence quenching as described in the Experimental section; (**B**) oxidative phosphorylation-dependent growth in sodium succinate minimal liquid medium at 37 °C was determined by measuring the D_{650} of the culture at maximal density. The maximal density of the βFLAG/ΔCys strain corresponded to $D_{650} = 0.90$ (minimum of two trials). All values are reported as a percentage of the βFLAG/ΔCys enzyme or strain. The squares indicate results from the deleterious *a*R210C, *a*G213C, *a*G218C and *a*E219C mutant membranes.

Table 1 NADH-driven H^+ pumping in F_1-depleted membranes with deleterious subunit *a* helix 4 replacements

H^+ pumping of F_1-depleted membranes [42] was determined at 25 °C with 0.2 mg of membrane protein suspended in 2 ml of 10 mM Hepes/300 mM KCl/5 mM $MgCl_2$/1 μM Acridine Orange/1 μg/ml valinomycin (pH 7.5). Values are reported as percentages of maximal quenching of Acridine Orange fluorescence on the addition of NADH; 100% fluorescence was obtained after the addition of the protonophore CCCP (1 μM) (average of a minimum of two trials each). For each preparation, more than 95% of membrane-associated ATPase activity was removed.

Strain DK8/pACWU1.2	Quenching of total fluorescence (%)
βFLAG/WT	5
βFLAG/ΔCys	4
*a*R210C	74
*a*G213C	78
*a*G218C	21
*a*E219C	67

Not shown previously, however, were the deleterious effects of an *a*Gly-213 substitution. Membrane vesicles, which were not leaky to H^+ as demonstrated by the ability to form a ΔpH with NADH, showed no ATP-dependent H^+ pumping, even though the strain grew to 64% of the parental ΔCys strain (compare Figures 1A and 1B). Furthermore, the *a*G213C mutant membranes that were stripped of the F_1 complex developed an NADH-driven H^+ gradient similar to the other deleterious mutants, such as *a*R210C, indicating that the transport mechanism was perturbed (Table 1). In these experiments, more than 95% of membrane-associated ATPase activity was removed before assaying H^+ transport. Because *a*Gly-213, a non-conserved amino acid, is less than one turn of an α-helix from the essential *a*Arg-210, we decided to characterize further substitutions of this residue for perturbations of the transport mechanism.

Some *a*Gly-213 substitutions cause slow oxidative phosphorylation-dependent growth

Again with the DK8/pACWU1.2 expression system, *a*Gly-213 was replaced with Ser, Thr, Leu or Asn in an F_oF_1 background replete with native cysteine residues. Strains carrying the mutant plasmids had greatly increased doubling times relative to wild-type in oxidative phosphorylation-dependent growth. For example, DK8/pACWU1.2-*a*G213N had a doubling time of approx. 7 h in liquid sodium succinate medium at 37 °C compared with 1 h for the wild type (results not shown). In contrast, another mutant, *a*Gly-213 to Ser, grew on succinate similarly to the wild type.

Table 2 Characteristics of *a*Gly213 mutant strains

All values are averages of at least two experimental trials. F_oF_1 in membranes is expressed as a percentage of the mass of total protein in the membrane preparation. Each value is the average of at least two determinations. Quantification of the complex was performed as described in the Experimental section. The specific activity of ATPase in wild-type membranes was 5.30 μmol/min per mg of protein at 30 °C. The values for NADH-driven H^+ pumping reported were taken at the greatest extent of ACMA fluorescence quenching observed (see Figure 3). Note that these measurements were made with intact membranes.

Strain DK8/pACWU1.2	Growth on liquid succinate (% of wild-type)	F_oF_1 in membranes (% of total protein)	Membrane ATPase (% of wild-type)	NADH-driven H^+ pumping in intact membranes(% of wild-type)
Wild-type	100	13.9	100	100
*a*G213S	96	ND	44	91
*a*G213T	84	10.9	14	89
*a*G213C	70	8.7	11	105
*a*G213L	52	10.8	11	88
*a*G213N	55	15.0	10	97

Table 3 Characteristics of *a*G213N suppressor strains

Catalytic activities were measured as described in the Experimental section. k_{cat} values were calculated by using the amount of F_oF_1 complex in membrane preparations as determined by quantitative immunoblots. All values are the averages of triplicates.

		k_{cat} (s^{-1})		
Strain DK8/pACWU1.2	Diameter of colony on solid succinate(mm)	ATP hydrolysis	ATP synthesis	Synthesis/hydrolysis
Wild-type	0.55 ± 0.08	337	25.3	0.075
*a*G213N	0.011 ± 0.002	23	0.8	0.035
*a*G213N/*c*D61E	0.51 ± 0.11	104	8.3	0.080
*a*G213N/*a*L251V	0.098 ± 0.01	29	2.5	0.086
*a*G213N/*a*L251V/*c*D61E	0.59 ± 0.08	67	6.4	0.096

Interestingly, despite the slow growth, maximum growth yields were substantial (Table 2). Even the *a*G213N and *a*G213L mutants had growth yields more than 50% of the wild type. To assure that the growth yields were not due to genetic reversion, the plasmid was recovered at the end of growth from the *a*G213N strain and subjected to DNA sequencing through *uncB* and *uncE* (*a* and *c* subunits). The original mutation was present and no others were found, thus indicating that the slow but steady growth in liquid medium was a property of the *a*G213N mutation. These results suggested that *a*Gly-213 mutant strains retained at least a low level of ATP synthesis activity *in vivo*. Colony size on solid succinate medium was more reflective of the doubling times. Colonies of DK8/pACWU1.2/*a*G213N were only 0.011 ± 0.002 mm (mean $\pm$ S.D., $n = 10$) in diameter after 3 days at 37 °C in comparison with 0.55 ± 0.08 mm for the strain carrying the wild-type construct (Table 3).

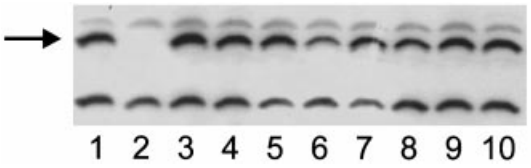

Figure 2 Immunoblot detection of mutant subunit *a*

SDS/PAGE [15% (w/v) gel] was used to separate 20 μg of membrane protein from various *E. coli uncB* mutants. After transfer to a PVDF membrane (Immobilon-P; Millipore, Bedford, MA, U.S.A.), the blot was reacted with a 1:2500 dilution of the rabbit polyclonal antiserum made against whole subunit *a* [56]. After washing, the peroxidase-conjugated anti-rabbit IgG secondary antibody (Roche Molecular Biochemicals) was added and the bands were detected with the Amersham ECL® kit. Lanes 1 and 10, membrane protein from strain DK8/pACWU1.2 (wild-type); lane 2, DK8/pBR322 (no F_oF_1 ATP synthase); lane 3, DK8/pACWU1.2/*a*G213N; lane 4, *a*G213N/*c*D61E; lane 5, *a*G213N/*a*L251V; lane 6, *a*G213N/*a*L251V/*c*D61E; lane 7, *c*D61E; lane 8, *a*L251V; lane 9, *a*L251V/*c*D61E. The arrow indicates the subunit *a* band, which is missing from the DK8/pBR322 sample (lane 2).

Properties of the *a*Gly-213 and suppressor mutants

As indicated in Table 2, membrane preparations containing the *a*G213T, *a*G213C, *a*G213L and *a*G213N mutant enzymes had low steady-state ATP hydrolytic rates approx. 10% of those of wild-type membranes. The mutant membranes contained amounts of F_oF_1 complex, including subunit *a* (Figure 2), and were able to generate NADH-driven ΔpH (Table 2), very similar to the wild type. Clearly, the replacement of Gly-213 does not create assembly mutants. ATP-dependent proton transport was also greatly attenuated in membrane vesicles from mutant strains. When Acridine Orange fluorescence was used to monitor the formation of a pH gradient at pH 7.5, no proton pumping was detected for the Cys, Leu and Asn mutant enzymes (results not shown). We observed previously that membranes made from strain DK8 had a significant rate of intrinsic proton leak that would short-circuit a low level of proton transport [49]. In efforts to circumvent this problem, we increased the sensitivity of the assay by using a pH 8.0 buffer and the dye ACMA to monitor the formation of the ΔpH (Figure 3A). Under these conditions, a transient low-level proton gradient was observed in the *a*G213T, *a*G213C and *a*G213L mutant membranes. Still no formation of a ΔpH was observed with the *a*G213N mutant membranes. It was conceivable that the *a*G213N mutant was completely incapable of ATP-dependent transport while retaining a low level of ATP synthesis activity, as demonstrated by the slow growth

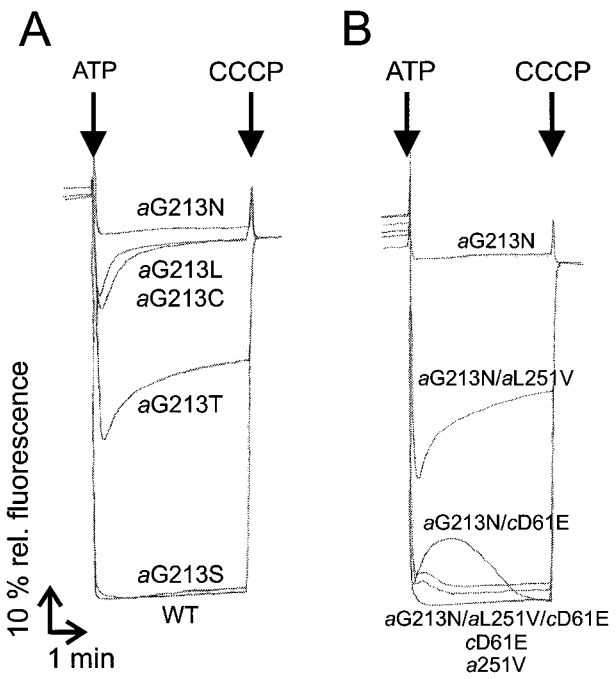

Figure 3 Formation of a ΔpH driven by ATP, monitored by ACMA

Membrane protein (0.25 mg) was suspended in 1 ml of 10 mM Hepes/300 mM KCl/5 mM $MgCl_2$/1 μM ACMA (pH 8.0); 1 μg/ml valinomycin in ethanol was added. The reactions were started with the addition of 1 mM ATP and terminated with the protonophore CCCP (1 μM). Fluorescence was monitored at 485 nm, with excitation at 415 nm. (**A**) Primary mutants of *a*Gly-213; (**B**) suppressor mutants of *a*G213N.

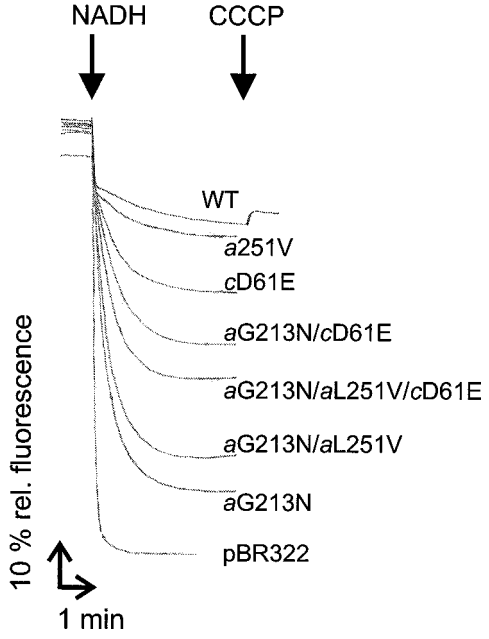

Figure 4 Formation of a ΔpH in stripped membranes driven by NADH

Membranes from the indicated strains were treated in low-ionic-strength buffer plus EDTA to remove F_1 complexes (see the Experimental section) [42]. In each case, more than 95% of F_1 was removed, as measured by residual ATPase activity. Stripped membranes (0.10 mg) were incubated in 1.0 ml of 10 mM Hepes/300 mM KCl/5 mM $MgCl_2$/1 μM Acridine Orange (pH 7.5) with the addition of 1 μg of valinomycin. The reactions were started with addition of 1 mM NADH and terminated with the addition of 1 μM CCCP. Emission was monitored at 530 nm, with excitation at 460 nm.

on succinate and by direct measurement of $\Delta\mu_H+$-dependent ATP synthesis (see the next section). However, because of the low activity and intrinsic proton leak of the membrane vesicles, it was more likely that a low level of proton pumping was below the limit of detection in our experimental system.

*a*G213N mutant is capable of net ATP synthesis

In spite of the intrinsic proton leak, the electron transport chain has excess capacity and is able to drive the maximal electrochemical gradient of protons, unless there is an additional leak [45]. Because the *a*G213N mutant strain was capable of oxidative phosphorylation-dependent growth, the mutant enzyme must have had at least a low level of activity. We hypothesized that the low activity in the form of proton pumping activity was unable to overcome the leak rate but would show net ATP synthesis when presented with substrates and an electrochemical gradient of protons near the static head level. In measuring NADH-driven ATP synthesis *in vitro*, we found that the *a*G213N mutant enzyme catalysed a low but significant level of net ATP synthesis with a k_{cat} that was 3 % of that of the wild type (Table 3). These results indicated that transport and catalysis of the *a*G213N mutant enzyme were coupled.

The efficiency of coupling was also assessed. To do this, we recalled that an efficiently coupled system requires that the catalytic mechanism be under thermodynamic and kinetic control of the transport mechanism [50–52]. In this case, a transport defect would be expected to attenuate the hydrolytic and synthetic reactions equally. A comparison of the ratio of the k_{cat} for synthesis and hydrolysis showed that the *a*G213N mutant enzyme was approximately half that of the wild type (0.035 for *a*G213N, compared with 0.075 for the wild type) (Table 3). The lower ratio suggested that the hydrolytic reaction was not as tightly regulated by transport and that transport was less effectively coupled to catalysis for ATP synthesis. In other words, catalysis and transport were less efficiently linked in the *a*G213N mutant complex.

*a*Gly-213 mutations cause defects in the transport mechanism

In addition to its effect on coupling efficiency, the *a*G213N and other *a*Gly-213 replacements greatly attenuated the ATP hydrolytic reaction. The lower catalytic rates were not due to defects in the F_1 sector because ATPase activities of F_1 released from the mutant membranes were the same as in the wild type (results not shown). Therefore the effects of the *a*Gly-213 mutations were due to perturbations of the transport process that were transmitted through coupling to the catalytic mechanism. To demonstrate the transport defect, passive proton conductance through F_o was assessed in mutant membranes that had been stripped of F_1. By incubation in a low-ionic-strength buffer in the presence of EDTA, more than 95 % of the F_1 sectors were removed as determined by the amount of ATPase activity associated with membranes. The ability to form an NADH-driven ΔpH was measured by Acridine Orange fluorescence quenching at pH 7.5 (Figure 4). The wild-type control showed enough passive leak to short-circuit proton pumping almost completely by electron transport. In contrast, the absence of the ATP synthase complex from the DK8/pBR322 control allowed a maximal gradient to form. The *a*G213N mutant F_o was clearly defective in mediating passive proton flux, although there seems to have been a small conductance.

Table 4 Transition-state thermodynamic parameters at 30 °C of subunit *a* mutant enzymes

Values are based on k_{cat} determined for each membrane preparation. k_{cat} values are listed in Table 3. The k_{cat} for *a*L251V was 177 s^{-1} at 30 °C; that for *c*D61E was 74 s^{-1} at 30 °C. ΔΔ values are the differences between the parameters for the mutants and those for the wild-type.

Strain DK8/pACWU1.2	$\Delta H‡$ (kJ/mol)	$\Delta\Delta H‡$ (kJ/mol)	$T(\Delta S‡)$ (kJ/mol)	$\Delta T(\Delta S‡)$ (kJ/mol)	$\Delta G‡$ (kJ/mol)	$\Delta\Delta G‡$ (kJ/mol)
Wild-type	35	–	−25	–	60	–
*a*G213N	77	42	10	35	67	7
*a*G213N/*a*L251V	71	36	5	30	66	6
*a*G213N/*c*D61E	65	30	2	27	63	3
*a*G213N/*a*L251V/*c*D61E	64	29	1	26	63	3
*a*L251V	54	19	−7	18	61	1
*c*D61E	74	39	10	35	64	4

Effects of *a*G213N are suppressed by mutations affecting transport-relevant residues

The extremely slow growth on solid succinate medium allowed us to screen for second-site suppressor mutations. We used a region-specific mutagenesis approach incorporating doped oligonucleotides in site-directed mutagenesis protocols (see the Experimental section) [42]. We focused our search for suppressor mutations in the C-terminal region of subunit *a* by using an oligonucleotide corresponding to residues *a*Leu-237 to *a*Leu-264. For subunit *c*, we used oligonucleotides corresponding to *c*Leu-4 to *c*Ile-30, *c*Leu-31 to *c*Thr-51 and *c*Gln-52 to *c*Ala-79. From screening 10^3–10^4 transformants from each mutagenesis reaction, two strains arose on solid succinate medium. DNA sequencing revealed that one had a mutation in codon 251 of subunit *a*, **C**TG → **G**TG, which resulted in a replacement of *a*Leu-251 with Val, and the other had a base change in codon 61 of subunit *c*, GA**T** → GA**A**, giving the replacement of *c*Asp-61 with Glu. The suppression of *a*G213N was confirmed by isolating DNA fragments containing these mutations, ligating into the original pACWU1.2/*a*G213N plasmid and testing the phenotype on succinate medium. As detailed in Table 3, the *a*L251V and, even more so, the *c*D61E second-site suppressor mutations conferred improved growth on succinate plates. These results suggested the functional linkage of the transport-essential carboxylic acid *c*Asp-61 to *a*Arg-210 and *a*Gln-252 because of their proximity to *a*Gly-213 and *a*Leu-251.

To different degrees, the *a*L251V and *c*D61E suppressor mutations restored ATP-dependent proton transport to the *a*G213N mutant (Figure 3B). Consistent with the succinate growth results was the observation that the *a*G213N/*c*D61E double mutant and the *a*G213N/*a*L251V/*c*D61E triple mutant showed higher transport activity than *a*G213N/*a*L251V. The increased activity was due to return of function and not to increased levels of subunit *a*. Immunoblot analysis showed that the amount of subunit *a* in the various complexes was constant (Figure 2). We note that the use of ACMA at pH 8.0 is more sensitive but that this assay also saturates at lower ΔpH. For example, the *a*L251V and *c*D61E single-mutant enzymes seemed to have similar activities to the wild type. However, in the less sensitive assay with Acridine Orange at pH 7.5, the *a*L251V enzyme had proton pumping similar to that of the wild type, whereas proton pumping of the *c*D61E enzyme was 10 % of that of the wild type (results not shown). Control experiments showed that membrane vesicles from each of the above strains formed NADH-driven proton gradients equal to those of the wild type.

As expected, the suppressor mutations *c*D61E and *a*L251V caused higher rates of ATP synthesis when combined with *a*G213N. Significantly, the ratios of synthesis to hydrolysis were also higher. As listed in Table 3, the ratios for both double mutants, as well as for the triple mutant *a*G213N/*a*L251V/*c*D61E, were similar to that of the wild type and more than twice that of *a*G213N alone. These results show that the effect of the suppressor mutations was, at least in part, to restore efficient coupling to the *a*G213N enzyme.

Whereas the *c*D61E suppressor mutation restored considerable proton transport function to *a*G213N, the *a*L251V suppressor did not (Figure 4). Taken together, the results indicate that the suppressor effect of *a*L251V was to restore efficient coupling as opposed to increasing turnover in F_o. Additionally, the turnover for ATP hydrolysis of the *a*G213N/*a*L251V double mutant was similar to that of *a*G213N alone (Table 3).

Effects of the *a*G213N transport mutants on the thermodynamic parameters of catalysis

We have previously used Arrhenius analyses of the catalytic transition state of steady-state ATP hydrolysis to assess the effects of amino acid replacements in the F_1 sector on the catalytic mechanism [42,43,45,49]. These analyses have been especially revealing with respect to the functional and physical interactions between the rotor γ subunit and the stator α and β subunits as well as an amino acid change at the γ–*c* subunit interface, γE208K, that affected coupling efficiency [49].

The amino acid substitutions described here also affected the catalytic transition state. The *a*G213N mutant enzyme showed large increases in the transition-state enthalpic and entropic parameters for steady-state ATP hydrolytic activity, which together added to a small change in the free energy (Table 4). The suppressor mutation *c*D61E, which resulted in significantly higher turnover rates for both ATP synthesis and proton transport when combined with *a*G213N, imparted lower $\Delta\Delta H^‡$ and $\Delta(T\Delta S^‡)$ values than for *a*G213N alone. In contrast, the *a*L251V mutations had small effects on catalytic and transport turnover as well as on the transition-state thermodynamic parameters. This correlation indicates that perturbations in the transport mechanism directly modulate the catalytic transition state and the rate-limiting step of steady-state activity.

DISCUSSION

The replacement of *a*Gly-213 with Asn had at least two effects. First, it decreased the turnover rate of proton transport as denoted by greatly attenuated ATP-dependent proton pumping, ATP hydrolysis, ATP synthesis and passive proton translocation. Secondly, the coupling efficiency was decreased by more than half compared with that of the wild-type enzyme. The suppressor mutations distinguished between the two effects. Both *a*L251V

and *c*D61E restored efficient coupling between transport and catalysis but only *c*D61E significantly increased the turnover rates of coupled active transport.

Because *a*G213N did not cause assembly defects as denoted by the presence of the complex, including subunit *a*, in the membranes at wild-type levels and the formation of a normal NADH-driven ΔpH gradient, the amino acid substitution probably did not cause global conformational perturbations. Instead, the suppression of *a*G213N by mis-sense mutations in two distinct positions suggested that the perturbation was localized. Consistent with *a*Gly-213 not being absolutely conserved was the observation that not all substitutions had deleterious effects (e.g. *a*G213S). Because a variety of amino acid side chains at position *a*213 (Cys, Thr, Leu and Asn) had similar effects, we suggest that the effects are indirect and mediated through another functional group. The obvious candidate is the essential *a*Arg-210. The spacing of three residues in an α-helix predicts that *a*Arg-210 is proximal to *a*Gly-213. The introduction of a larger group can change the environment or conformation of *a*Arg-210, perhaps causing the sub-optimal positioning of the guanidino moiety. The notion that the functional effects of the *a*Gly-213 mutations are caused indirectly through *a*Arg-210 is further supported by the *a*L251V suppressor mutation, which is adjacent to *a*Gln-252. If it is recalled that a double mutation, *a*R210Q/*a*Q252R, retained a low level of coupled transport [28], this indicates strongly that *a*Arg-210 and *a*Gln-252 are spatially close. We suggest that *a*L251V suppresses the effects of *a*G213N by allowing *a*Arg-210 to regain, in part, its wild-type conformation or environment.

The same considerations can be made for the other *a*G213N suppressor, *c*D61E. The carboxylic acid is also probably spatially close to *a*Arg-210 because cysteine cross-links between subunits *a* and *c*, in particular between positions *a*214 and *c*62, indicate the proximity of the transmembrane helices containing these residues [33]. The suppression of *a*G213N by *c*D61E reinforces this conclusion. Our results provide, for the first time, functional evidence supporting various models [10,12,16,18,28,29] that suggest a direct interaction between the critical transport residues, *a*Arg-210 and *c*Asp-61. These residues, along with *a*Gln-252, which is an important but not essential component, constitute the 'transport site'. The fact that amino acid substitutions of both *a*G213N suppressor mutations, *a*L251V and *c*D61E, differed from the wild-type residues by only one methylene group suggests the precise structural arrangement of residues in the site.

In each of the transport mechanism models, the guanidino group of the Arg is believed to lower the p*K* of *c*Asp-61, forcing deprotonation, or to form a transient hydrogen bond. It is apparent that perturbation of this interaction not only decreases the turnover rate of coupled transport but also decreases coupling efficiency. This latter role implies that the coupling mechanism involves the transmission of conformational information to and from the transport site, which is important for maximum efficiency and minimal slippage in the coupling mechanism. Evidence for conformational coupling is suggested by differences in the solution structures of the protonated compared with the unprotonated *c* subunit [10]. Its polar loop, through which coupling is mediated via contacts with the ε [53] and γ [42] subunits, has distinct differences in conformation. The direct structural interactions between the *c* polar loop and the ε (δ in mitochondrial nomenclature) and γ subunits have recently been confirmed by the crystal structure of the yeast F_oF_1 complex [11].

Analysis of the catalytic parameters in complexes with transport mutations provides information on the mechanism of coupling. We have shown previously that amino acid substitutions that affect coupling and do not directly perturb the catalytic mechanism can significantly influence the transition-state thermodynamic parameters. For example, the catalytic mechanism of the mutant γE208K enzyme was effectively uncoupled from transport at temperatures above approx. 30 °C [42] and had a significant increase in the transition-state enthalpic and entropic parameters. The increase in the transition-state thermodynamic parameters was reversed when the mutant F_1 was released from F_o. When free of the influence of F_o and the transport mechanism, the mutant γE208K F_1 had identical parameters to those of wild-type F_1.

In contrast with the γE208K mutation, the mutations of *a*Gly-213 retained coupling, albeit less efficiently in *a*G213N. An excellent and unique example of a transport mutant that exclusively attenuates catalysis via coupling is *a*G213N/*a*L251V. In this case, the low turnover in transport had a strong kinetic effect on catalysis. Its k_{cat} was less than 10% of that of the wild type; the large increase in $\Delta H^{\ddagger}$ and $\Delta S^{\ddagger}$ remained virtually as high as that in the single mutant *a*G213N. Clearly, the slow catalytic turnover of the *a*G213N and *a*G213N/*a*L251V enzymes is linked to the slow turnover of transport. The lower turnover is reflected in the much larger activation energy, E_a, that must be overcome to reach the catalytic transition state (Table 4), which by definition is the rate-limiting step.

We point out that not all amino acid substitutions that have functional perturbations cause positive changes in the transition-state enthalpic and entropic parameters. For example, some amino acid replacements in the interaction region between the $\beta D^{380}ELSEED^{386}$ segment and the γ subunit have the opposite effect. Mutations such as βE381K or γR242E decrease $\Delta H^{\ddagger}$ and $\Delta S^{\ddagger}$ and generally cause destabilization of the complex [49]. Furthermore, analysis of a multitude of mutant enzymes that have no differences in catalytic or transport characteristics from those of the wild type have unaltered transition-state thermodynamic parameters (results not shown). We also point out that effects on the thermodynamic parameters of catalysis are easily missed if the level of wild-type and mutant activity happen to coincide near the assay temperature. For example, the ATPase activity of γM23K F_1 is the same as that of wild-type F_1 at 21 °C; however, the $\Delta H^{\ddagger}$ of the γM23K enzyme is 22 kJ/mol greater [43].

We can use the transition-state thermodynamic parameters to provide information on the coupling of transport to the catalytic mechanism. For a given reaction series that uses the same transition state there should be a quantitative relationship between enthalpy and entropy of activation, such as an isokinetic relationship [54]. We previously demonstrated that the transition-state thermodynamic parameters from ATP synthases with a variety of mutations or from different sources could be fitted to an isokinetic line [43,45] such as that shown in Figure 5. In isokinetic relationships there is a linear free-energy relationship between two rate constants (k_1 and k_2) measured at two temperatures ($T_2 > T_1$), which can be given by the equation:

$$\log k_2 = a + b \log k_1$$

where *a* and *b* are constants [54]. In a stringent test of an isokinetic relationship, Figure 5 shows that there are excellent linear correlations between experimental rate constants derived at three different temperatures (25, 30 and 35 °C) compared with rate constants determined at 20 °C. Additional verification of the relationship has been given previously [45]. These analyses confidently indicate that each of the enzymes conforming to the linear relationship share the same transition-state structure and therefore have the same rate-limiting step. The mutations in subunits *a* and *c* described here clearly fall on the regression lines (Figure 5). The points falling at the extreme of the plot belong to

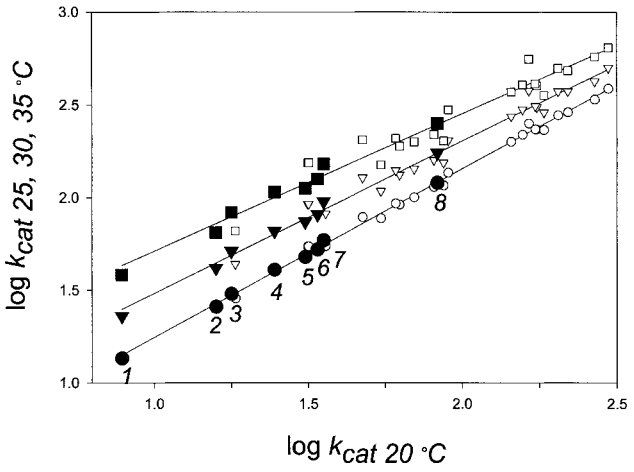

Figure 5 Isokinetic plot of mutant F_0F_1 enzymes

A plot of k_{cat} at 20 °C against k_{cat} is shown for an enzyme at 25 °C (○,●), 30 °C (▽,▼), or 35 °C (□,■). The correlation coefficient ranged from $r^2 = 0.96$ to $r^2 = 0.99$. The large filled points (●,▼,■) represent the value sets for the mutant enzymes presented here and are numbered as follows: 1, *a*G213N; 2, *a*G213L; 3, *c*D61E; 4, *a*G213C; 5, *a*G213N/*a*L251V; 6, *a*G213N/*a*L251V/*c*D61E; 7, *a*G213N/*c*D61E; 8, *a*L251V. See Al-Shawi et al. [43,45,57] for the other mutants plotted and for more detailed discussion.

the *a*G213N mutant, emphasizing the large effect that this transport mutant has on the catalytic transition state. We have previously argued that the rate-limiting step of both ATP hydrolysis and synthesis involves rotation of the γ subunit relative to the $\alpha_3\beta_3$ hexamer [45]. Because the transport mutants have altered thermodynamic parameters of steady-state activity, transport is coupled to the rate-limiting step, or the rotation of the γ subunit.

According to transition-state theory, the increase in the transition-state enthalpic and entropic parameters suggests that there are extra bonds that must be broken to reach the rate-limiting transition state. Because of the spatial proximity of *a*Gly-213 and *a*Arg-210, we suggest that the *a*G213N and *a*G213L mutations cause *a*Arg-210 to strengthen existing interactions or to form new ones, possibly with *c*Asp-61, that must be broken before the enzyme can proceed through its reaction cycle. This effect might involve the steps of protonation or deprotonation of *c*Asp-61 or the rotation of *c*Asp-61 past *a*Arg-210 [16]. A larger activation energy for transport is expected if, for example, the p*K* of *c*Asp-61 has shifted, thus affecting the rate-limiting transition state for the transport of each proton. The unusually large increase in the transition-state activation energy might indicate an additive property of the transport mechanism. Assuming a stoichiometry of four protons per ATP, the *a*G213N mutant enzyme must overcome extra interactions, possibly between *a* and *c* subunits, for each proton translocated and four times for each ATP hydrolysed or synthesized. Thus the higher activation energy in transport is manifested as a surprisingly large activation energy of the catalytic transition state and much lower turnover for transport and therefore catalysis.

Moreover, the effects of the *a*G213N mutation are consistent with the transport step's involving a conformational change that transverses the entire complex to the catalytic domain [19]. Several mutations in key positions that block the transmission of conformational information have been identified. Amino acid substitutions in the interfaces between the β and γ subunits [43,49], the ϵ and *c* subunits [53], the ϵ and *a* subunits [55] and the γ and *c* subunits [42] perturb proper transmission and result in inefficient coupling.

This work was supported by Public Health Service grant GM50957 to R.K.N.; P.H.K. was supported by MSTP training grant GM07267.

REFERENCES

1 Deckers-Hebestreit, G. and Altendorf, K. (1996) Annu. Rev. Microbiol. **50**, 791–824
2 Boyer, P. D. (1997) Annu. Rev. Biochem. **66**, 717–749
3 Weber, J. and Senior, A. E. (1997) Biochim. Biophys. Acta **1319**, 19–58
4 Nakamoto, R. K., Ketchum, C. J. and Al-Shawi, M. K. (1999) Annu. Rev. Biophys. Biomol. Struct. **28**, 205–234
5 Abrahams, J. P., Leslie, A. G. W., Lutter, R. and Walker, J. E. (1994) Nature (London) **370**, 621–628
6 Duncan, T. M., Bulygin, V. V., Zhou, Y., Hutcheon, M. L. and Cross, R. L. (1995) Proc. Natl. Acad. Sci. U.S.A. **92**, 10964–10968
7 Sabbert, D., Engelbrecht, S. and Junge, W. (1996) Nature (London) **381**, 623–625
8 Noji, H., Yasuda, R., Yoshida, M. and Kinosita, K. (1997) Nature (London) **386**, 299–302
9 Yasuda, R., Noji, H., Kinosita, K. and Yoshida, M. (1998) Cell **93**, 1117–1124
10 Rastogi, V. K. and Girvin, M. E. (1999) Nature (London) **402**, 263–268
11 Stock, D., Leslie, A. G. W. and Walker, J. E. (1999) Science **286**, 1700–1705
12 Vik, S. B. and Antonio, B. J. (1994) J. Biol. Chem. **269**, 30364–30369
13 Groth, G. and Walker, J. E. (1997) FEBS Lett. **410**, 117–123
14 Girvin, M. E., Rastogi, V. K., Abildgaard, F., Markley, J. L. and Fillingame, R. H. (1998) Biochemistry **37**, 8817–8824
15 Sambongi, Y., Iko, Y., Tanabe, M., Omote, H., Iwamoto-Kihara, A., Ueda, I., Yanagida, T., Wada, Y. and Futai, M. (1999) Science **286**, 1722–1724
16 Elston, T., Wang, H. and Oster, G. (1998) Nature (London) **391**, 510–513
17 Junge, W., Lill, H. and Engelbrecht, S. (1997) Trends Biochem. Sci. **263**, 420–423
18 Kaim, G., Matthey, U. and Dimroth, P. (1998) EMBO J. **17**, 688–695
19 Fillingame, R. H. (1990) in The Bacteria, vol. 12, (Krulwich, T. A., ed.), pp. 345–391, Academic Press, New York
20 Miller, M. J., Oldenburg, M. and Fillingame, R. H. (1990) Proc. Natl. Acad. Sci. U.S.A. **87**, 4900–4904
21 Fraga, D., Hermolin, J. and Fillingame, R. H. (1994) J. Biol. Chem. **269**, 2562–2567
22 Zhang, Y. and Fillingame, R. H. (1994) J. Biol. Chem. **269**, 5473–5479
23 Zhang, Y. and Fillingame, R. H. (1995) J. Biol. Chem. **270**, 87–93
24 Assadi-Porter, R. M. and Fillingame, R. H. (1995) Biochemistry **34**, 16186–16193
25 Kaim, G. and Dimroth, P. (1998) Biochemistry **37**, 4626–4634
26 Lightowlers, R. N., Howitt, S. M., Hatch, L., Gibson, F. and Cox, G. B. (1987) Biochim. Biophys. Acta **894**, 399–406
27 Cain, B. D. and Simoni, R. D. (1989) J. Biol. Chem. **264**, 3292–3300
28 Hatch, L. P., Cox, G. B. and Howitt, S. M. (1995) J. Biol. Chem. **270**, 29407–29412
29 Valiyaveetil, F. L. and Fillingame, R. H. (1997) J. Biol. Chem. **272**, 32635–32641
30 Hartzog, P. E. and Cain, B. D. (1993) J. Bacteriol. **175**, 1337–1343
31 Long, J. C., Wang, S. and Vik, S. B. (1998) J. Biol. Chem. **273**, 16235–16240
32 Valiyaveetil, F. I. and Fillingame, R. H. (1998) J. Biol. Chem. **273**, 16241–16247
33 Jiang, W. and Fillingame, R. H. (1998) J. Biol. Chem. **95**, 6607–6612
34 Kuo, P. H., Ketchum, C. J. and Nakamoto, R. K. (1998) FEBS Lett. **426**, 217–220
35 Klionsky, D. J., Brusilow, W. S. A. and Simoni, R. D. (1984) J. Bacteriol. **160**, 1055–1060
36 Moriyama, Y., Iwamoto, A., Hanada, H., Maeda, M. and Futai, M. (1991) J. Biol. Chem. **266**, 22141–22146
37 Zhou, Y., Duncan, T. M., Bulygin, V. V., Hutcheon, M. L. and Cross, R. L. (1996) Biochim. Biophys. Acta **1275**, 96–100
38 Sambrook, J., Fritsch, E. F. and Maniatis, T. (1989) Molecular Cloning: A Laboratory Manual, 2nd edn, Cold Spring Harbor Laboratory, Cold Spring Harbor, NY
39 Mullis, K. B., Ferré, F. and Gibbs, R. A. (1994) The Polymerase Chain Reaction, Birkhäuser, Boston
40 Futai, M., Sternweis, P. C. and Heppel, L. A. (1974) Proc. Natl. Acad. Sci. U.S.A. **71**, 2725–2729
41 Lowry, O. H., Rosebrough, N. J., Farr, A. L. and Randall, R. J. (1951) J. Biol. Chem. **193**, 265–275
42 Ketchum, C. J. and Nakamoto, R. K. (1998) J. Biol. Chem. **273**, 22292–22297
43 Al-Shawi, M. K., Ketchum, C. J. and Nakamoto, R. K. (1997) J. Biol. Chem. **272**, 2300–2306
44 Nakamoto, R. K., Al-Shawi, M. K. and Futai, M. (1995) J. Biol. Chem. **270**, 14042–14046
45 Al-Shawi, M. K., Ketchum, C. J. and Nakamoto, R. K. (1997) Biochemistry **36**, 12961–12969
46 Fabiato, A. and Fabiato, F. (1979) J. Physiol. (Paris) **75**, 463–505
47 Lightowlers, R. N., Howitt, S. M., Hatch, L., Gibson, F. and Cox, G. B. (1988) Biochim. Biophys. Acta **933**, 241–248

48 Hartzog, P. E. and Cain, B. D. (1994) J. Biol. Chem. **269**, 32313–32317
49 Ketchum, C. J., Al-Shawi, M. K. and Nakamoto, R. K. (1998) Biochem. J. **330**, 707–712
50 Jencks, W. P. (1980) Adv. Enzymol. **51**, 75–106
51 Tanford, C. (1983) Annu. Rev. Biochem. **52**, 379–409
52 Inesi, G., Lewis, D., Nikic, D., Hussain, A. and Kirtley, M. E. (1992) Adv. Enzymol. **65**, 185–215
53 Zhang, Y., Oldenburg, M. and Fillingame, R. H. (1994) J. Biol. Chem. **269**, 10221–10224
54 Exner, O. (1973) Prog. Phys. Org. Chem. **10**, 411–482
55 Gardner, J. L. and Cain, B. D. (1999) Arch. Biochem. Biophys. **361**, 302–308
56 Yamada, H., Moriyama, Y., Maeda, M. and Futai, M. (1996) FEBS Lett. **390**, 34–38
57 Al-Shawi, M. K., Parsonage, D. and Senior, A. E. (1990) J. Biol. Chem. **265**, 4402–4410

Received 3 December 1999/20 January 2000; accepted 22 February 2000